Effect of Treatment of Bis(3-triethoxysilyl propyl)tetrasulfane on Physical Property of *In Situ* Sodium Activated and Organomodified Bentonite Clay – SBR Rubber Nanocomposite

Sugata Chakraborty,[1] Saptarshi Kar,[1] Saikat Dasgupta,[1] Rabindra Mukhopadhyay,[1] Samar Bandyopadhyay,[2] Mangala Joshi,[3] Suresh C. Ameta[4]

[1]*Hari Shankar Singhania Elastomer and Tyre Research Institute (HASETRI), Rajsamand, Rajasthan 313 342, India*
[2]*R&D Centre, J.K. Tyre, Rajsamand, Rajasthan, India*
[3]*Department of Textile Technology, Indian Institute of Technology, Delhi 110016, India*
[4]*Department of Chemistry, Mohanlal Sukhadia University, Udaipur 313 001, Rajasthan, India*

Received 27 June 2009; accepted 2 October 2009
DOI 10.1002/app.31549
Published online 5 January 2010 in Wiley InterScience (www.interscience.wiley.com).

ABSTRACT: This study describes the effect of treatment of Bis(3-triethoxysilyl propyl)tetrasulfane (silane coupling agent, Si69, TESPT) on *in situ* sodium activated, organo modified bentonite clay – styrene butadiene rubber (SBR) nanocomposite. transmission electron microscopy and Wide angle X-ray diffraction indicated the intercalation as well as partial exfoliation in both the organoclay and silane treated organoclay compound. It was found that about 5% of silane with respect to clay was the optimum dose for the treatment. Around 15% improvement in tensile and tear strength was observed due to silane treatment. Silane treated organoclay exhibited substantial improvement of the fatigue life, compression set, and rebound property. A detailed study of physical property was carried out. A comparison with low and high structure carbon black filled compound was also carried out. It revealed that the silane treatment helped organoclay to achieve comparable property of the compound having equivalent carbon black loading. Probable mechanism of interaction of silane with clay has also been proposed. © 2010 Wiley Periodicals, Inc. J Appl Polym Sci 116: 1660–1670, 2010

Key words: nanocomposites; silane; organoclay; bentonite; SBR; rubber

INTRODUCTION

The polymer clay nanocomposites have gained attention from researchers due to three major advantages that nanocomposites have over conventional composite. They are lighter weight due to low filler loading, low cost due to fewer amounts of filler use, and improved properties (includes mechanical, thermal, optical, electrical barrier, etc.) compared to conventional composites at very low loading of filler. Polymer clay nanocomposites can be prepared by solution blending or direct intercalation or sol/gel technique or *in situ* polymerization or by latex blending.[1–12]

Due to easy availability of the different rubbers in latex form and swelling capability of the clay in the water, the mixing of the latex with the layered silicates (having high cation exchange capacity) followed by co-precipitation (coagulation) is a promising route for producing rubber nanocomposites.[13] Varghese and Karger-Kocsis[14] prepared NR based nanocomposites with 10 wt % natural (sodium bentonite) and synthetic (sodium fluorohectorite) layered silicates by the latex compounding method. Wang et al.[15] prepared NR-MMT and chloroprene rubber (CR)-MMT clay nanocomposites by co-coagulating the rubber latex and the aqueous clay suspension. Stephen et al.[16] studied the impact of layered silicates like sodium bentonite and sodium fluorohectorite on the rheological behavior of NR, carboxylated SBR (XSBR) lattices, and their blends with special reference to shear rate, temperature, and filler loading. Zhang et al.[17] prepared clay (natural clay fractionated from bentonite)-SBR nanocomposites by mixing the SBR latex with a clay/water dispersion and coagulating the mixture. Wang et al.[18] compared the mechanical properties of clay (fractionated bentonite)/SBR nanocomposites prepared by the solution and latex blending techniques and found that at equivalent clay loadings, the nanocomposites prepared by the latex route were better than those prepared by the solution blending technique. Jia et al.[12] combined *in situ* organic modification of MMT and the latex compounding method to prepare high performance SBR/MMT nanocomposites by improving the interfacial interaction between nano-dispersed layered clay and SBR.[12]

Correspondence to: S. Bandyopadhyay (sbanerjee@ktp.jkmail.com).

Applications of such rubber nanocomposites are contemplated, for example as tire tread and inner liner. However, some of the properties are seems to be inferior for rubber clay nanocomposites. It has been reported that with increase with nanoclay, the fatigue life of the compounds decreases.[19] Same type of observation has also been reported for rebound resilience property.[20] It is reported that at equivalent carbon black loading, the set property of the nanocomposites are inferior.[18]

Author's previous publication[21] deals with a novel single step method to form *in situ* sodium activation and organo modified bentonite clay – SBR rubber nanocomposites. In this study, effect of silane treatment on the physical property of *in situ* sodium activation and organo modified bentonite clay – SBR rubber nanocomposites has been evaluated. The properties have also been compared with low and high structure (N660 and N330) carbon black filled compounds at equivalent carbon black loading. A possible mechanism has also been proposed.

This kind of nanocomposites can be used in tyre tread, side wall or inner liner. Auto motive tube is also an area, where such kind of nanocomposites can play a crucial role due to its superior air retention property.

EXPERIMENTAL SECTION

Materials

The SBR latex (Encord 205) with 25% bound styrene and 40% solids content was supplied by M/S Jubilant Organosys (Borada, India). The Mooney viscosity (ML [1 + 4] at 100°C) of the coagulated SBR latex was 51. Apart from SBR latex, SBR 1502 (emulsion grade) from BST Elastomers (Bankok, Thailand bound styrene 24%, Mooney viscosity 50 (ML [1 + 4] at 100°C), volatile matter 0.02%, specific gravity 0.94) was also used in the compound formulations. Unpublished work in our laboratory indicates that the gum properties of both those SBRs are similar and thus SBR 1502 was used for dose adjustment during compound formulation as reported later. The clay used in this work is unfractionated bentonite clay available locally in Rajasthan, India.

The rubber compounding ingredients used in this work were of commercial grade, viz. zinc oxide, stearic acid, sulphur, N-t-butylbenzothiazole-2-sulphenamide (TBBS), and N660 and N330 carbon black. Bis(3-triethoxysilyl propyl)tetrasulfane (Silane) was purchased from Dugassa AG (Bitterfeld, Germany).

Synthesis of the *in situ* modified bentonite clay nanocomposite master batch

The synthesis of the *in situ* sodium activated and organomodified bentonite clay master batch was carried out according to the published literature.[21] About 10 g of the unfractionated pristine bentonite clay was dispersed in 500 mL of distilled water using a Remi (India) stirrer for 1 h at 2000–3000 rpm. The temperature was maintained to around 80°C. Next sodium chloride (10% with respect to clay) was added to the hot clay slurry. The slurry was further stirred for 4 h at 2000–3000 rpm and 80°C. Required amount of octadecyl amine (about 1.5 equivalent times of CEC of the clay) was stirred with equivalent amount of hydrochloric acid in distilled water at 80°C. The amine solution became colorless after some time. The amine solution was then added to the clay slurry and stirring was continued for another 2 h at 80°C and at 2000–3000 rpm. Diluted SBR latex (20% total solid) was then added to the aqueous slurry. The amount of latex was adjusted to make 20 parts of clay in 100 parts of rubber (i.e. 20 phr.) on dry basis. The pH of the solution was adjusted to around 3–4. The solid content of the slurry was finally maintained around 20–25%. The mixture was further stirred for another 1 h. The resultant solution was coagulated during stirring. The mass was washed several times with tap water and dried at 70°C in a hot air oven.

Compound mixing

The single stage mixing was done in a Brabender Plasticorder model PL 2000-3 (M/s Brabender, Germany) having a chamber volume of 80 cm^3, cam rotors, ram pressure weight of 5 kg and batch weight of 70 g.

Single stage mixing was carried out for 10 min using 60 rpm rotor speed at 70°C. Initially 1 min mastication time was allowed for the rubber. Then clay or clay master batch was added and mixed for 6 min. Finally, other ingredients were added and the batch dumped after 3 min.

For silane treatment, the mixing was carried out in three stages. In first stage, the rubber and the nanocomposite master batch was mixed for 4 min using 60 rpm rotor speed at 70°C. In second stage, 1 min mastication time was allowed for the first stage master batch rubber using 60 rpm rotor speed at 145°C. Then required amount of silane was added and further mixed for 2 min. In the third stage, 1 min mastication time was allowed for the second stage master batch using 60 rpm rotor speed at 70°C. Then required curatives were added and further mixed for 2 min.

The mixed batches were further milled on a laboratory two-roll mill from M/s Santosh Industries (India). The respective compound formulations are shown in Tables I and II.

The SBR dose was adjusted by adding SBR 1502 from outside during mixing.

TABLE I
Compound Formulation with Varying Dose of Silane

Material	$5A3Si_2$	$5A3Si_5$	$5A3Si_7$	$5A3Si_{10}$
SBR1502	100	100	100	100
Nano-clay (from nanocomposite master batch)	5	5	5	5
Silane	0.1	0.25	0.35	0.50
ZnO	3	3	3	3
TBBS	1	1	1	1
Stearic acid	1	1	1	1
Sulfur	1.75	1.75	1.75	1.75

Characterization of the SBR/bentonite clay nanocomposites

Wide angle X-ray diffraction (WAXD) measurements were carried out in a Philips 1710 X-ray diffractometer using a scan rate of 0.5°/min with Cu Kα target at 40 kV and 25 mA (wavelength = 0.154 nm) with 2θ scan range from 2 to 10°. The X-ray diffractograms are represented in Figure 1. The peak position and the corresponding spacing of the d_{001} plane is reported in Table III.

For transmission electron microscopy (TEM) measurements, 100 nm sections were microtomed at −120°C using Ultracut E ultramicrotome (Reichert and Jung) with a diamond knife. Measurements were carried out with a Philips CM200 TEM at an acceleration voltage of 120 kV. The TEM micrographs are given in Figures 2–5, respectively.

Energy dispersive X-ray spectrophotometry (EDS) study was carried out with the help of Quantax 200 with X-Flash liquid nitrogen free detector from Bruker, Germany for the elemental mapping of the samples. The aluminium mapping of the samples are reported in Figure 6.

The thermal stability of the cured samples was determined by carrying out thermogravimetric analysis (TGA) using Pyris-1 TGA of M/s Perkin Elmer (Shelton, USA). For each sample three tests were carried out under the same heating rate and the temperatures were reproducible to ±3.0°C. Initially the sample was heated under nitrogen atmosphere up to 600°C and then the gas was changed to oxygen and the heating continued up to 800°C. The heating rate was 40°C/min. The TGA and DTG thermograms are shown in Figures 7 and 8, respectively. The decomposition data are represented in Table IV.

Differential scanning calorimetry (DSC) experiments were performed in dynamic mode using Diamond DSC (Perkin Elmer, Norwalk, USA) to measure the glass transition temperature (T_g). The scanning rate was 20°C/min under nitrogen atmosphere. The DSC thermograms are shown in Figure 9 and T_g values are reported in Table V.

The rheometric properties were determined in a moving die rheometer (MDR 2000E) from M/s Alpha Technologies (Akron, USA) at 160°C for 30 min keeping the rotor arc at 0.5° in accordance with ASTM D 5289. Rheometric properties are reported in Tables VI and VII.

Curing of tensile slabs was done using a compression molding technique in an electrically heated curing press from M/s Hind Hydraulics (New Delhi, India) at 160°C for 30 min. The tensile samples were died out in accordance with ASTM D412 type C die.

The stress–strain properties were determined using a universal testing machine, Zwick UTM 1445 from M/s Zwick (Ulm, Germany) in accordance with ASTM D412. The hardness was determined in a Shore A durometer from M/s Prolific Industries (New Delhi, India) in accordance with ASTM D2240.

The tear properties were measured according to ASTM D624. The Mooney viscosity was measured using MV2000E from Alfa Technologies (Akron, USA) in accordance with ISO 289-1.

Cure rate index (CRI) was measured according to ASTM D5289. The following formula was used for the CRI in the study:

TABLE II
Formulation of Different Compounds

Material	B1	B2	10A3	$10A3Si_5$	$N10_{330}$	$N10_{660}$
SBR1502	100	100	100	100	100	100
Nano-clay (from nanocomposite master batch)	–	–	10	10	–	–
Silane	–	0.5	–	0.5	–	–
Bentonite clay	10	10	–	–	–	–
Carbon black, N330	–	–	–	–	10	–
Carbon black, N660	–	–	–	–	–	10
ZnO	3	3	3	3	3	3
TBBS	1	1	1	1	1	1
Stearic Acid	1	1	1	1	1	1
Sulfur	1.75	1.75	1.75	1.75	1.75	1.75

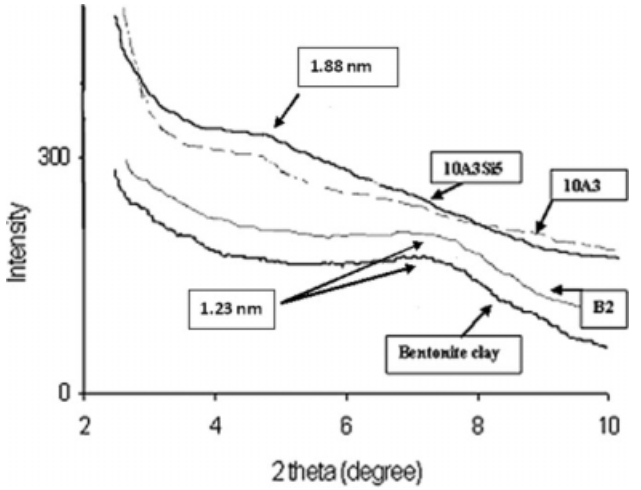

Figure 1 X-ray diffractogram of the compounds.

where,

$$\text{CRI} = \frac{100}{t_{c90} - t_{s2}} \quad (1)$$

The swelling index of the cured samples was measured using the following formula in accordance with ASTM D3616.

$$\text{Swelling index} = \frac{\text{Swollen weight}}{\text{Initial weight}} \quad (2)$$

Volume fraction was also performed to get an indication of apparent crosslink density. Weighed sample of cured rubber vulcanizate was immersed in toluene solvent for 48 h at room temperature. Excess solvent was then blotted from the sample and the swollen weight was measured. The swollen sample was dried in oven at 100°C till constant weight. Dried weight of the sample was taken after cooling the sample in the desiccators. The volume fraction, V_r[22] of the vulcanizate rubber was calculated using following formula:

$$V_r = \frac{(D - FT)/\rho_r}{(D - FT)/\rho_r + A_0/\rho_s} \quad (3)$$

where D is the weight of the deswollen sample; F is the weight fraction of the insoluble non-rubber ingredients; T is the original dry weight of the sample; A_0 is the weight of solvent absorbed; ρ_r is the density of the rubber (density value is 910 kg/m^3); and ρ_s is the density of the solvent (density value is 870 kg/m^3).

TABLE III
Thermogravimetric Data of Various Compounds

Sample	Decomposition up to 400°C (%)	Peak decomposition temperature (°C)	Peak decomposition rate (%/min)
10A3	8.8	498	33.0
10A3Si$_5$	8.8	500	33.1
B1	8.9	480	50.2
B2	9.0	481	50.5

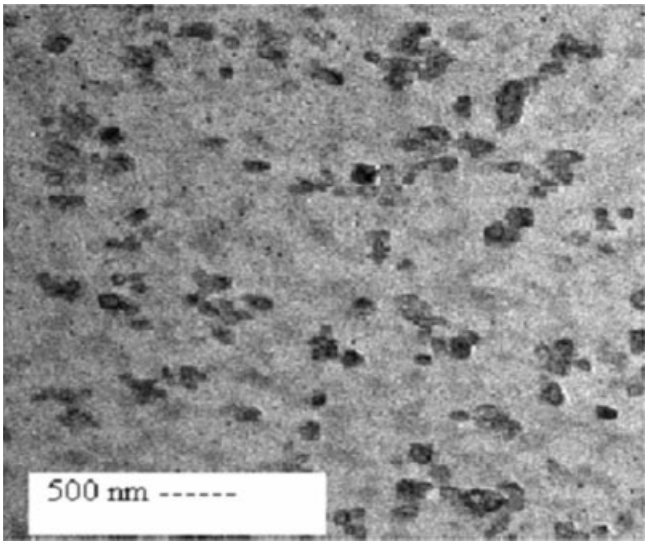

Figure 2 TEM image of compound 10A3 at low magnification.

Bound rubber content was also measured by using the following formula

$$\text{Bound rubber} = \frac{(M_B - M_F - M_D)}{M_B} \times 100\% \quad (4)$$

where M_B is the weight of the uncured mix before immersing in toluene, M_F is the weight of the filler

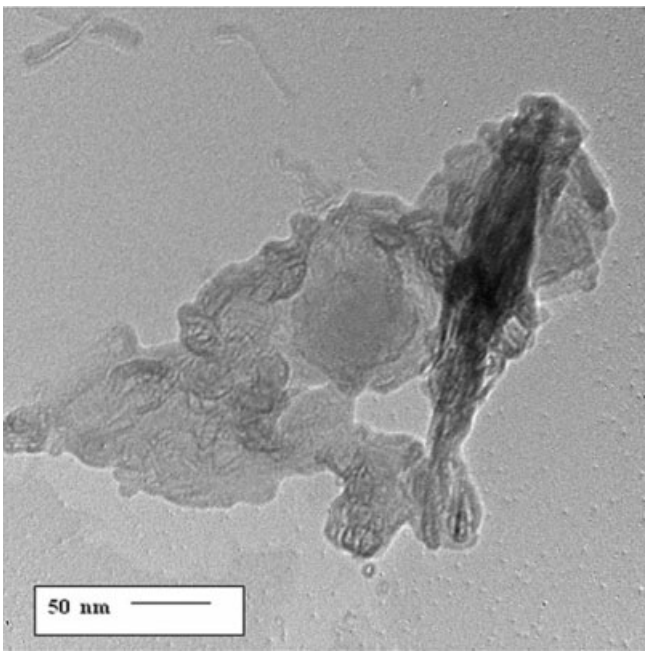

Figure 3 TEM image of compound 10A3 at high magnification.

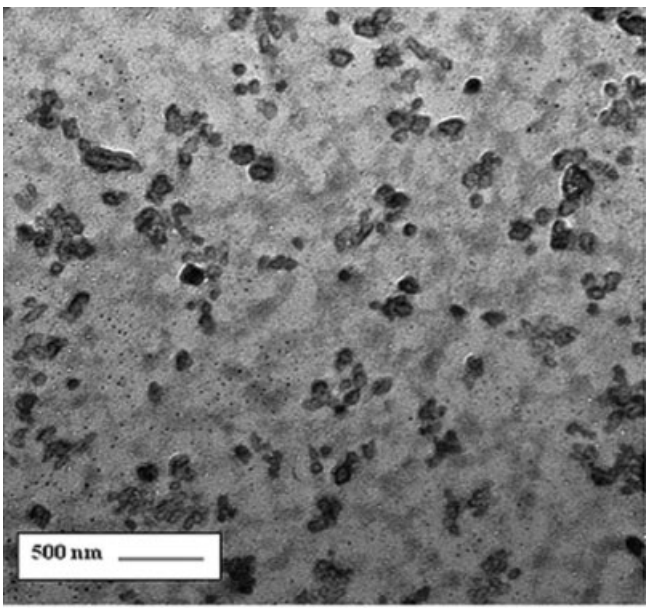

Figure 4 TEM image of compound 10A3 Si_5 at low magnification.

in the uncured mix (i.e M_B) and M_D is the weight of the rubber dissolve in the solvent.

Rebound resilience and compression set of samples were carried out according to ISO 4662 and ASTM D395, respectively.

The fatigue to failure properties (FTFT) at 100% extension ratio was measured in a Monsanto FTFT machine (ASTM D4482). The fatigue life was calculated using the Japanese Industrial Standard (JIS) average method.

Air permeability test was carried out according to ISO 2782.

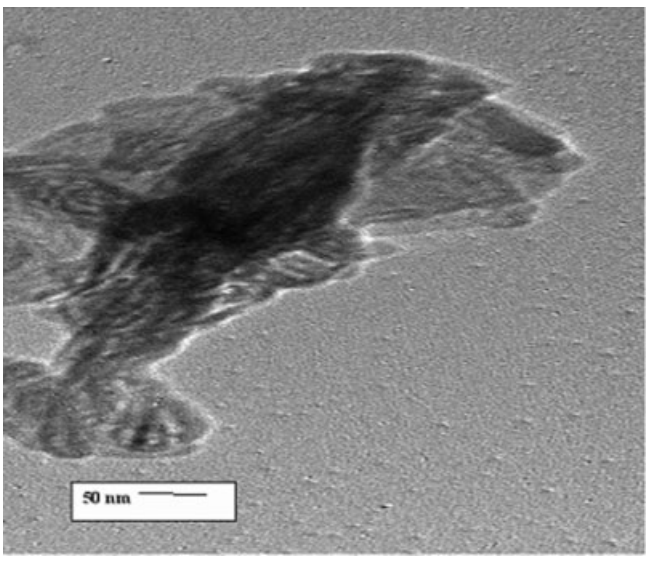

Figure 5 TEM image of compound 10A3 Si_5 at high magnification.

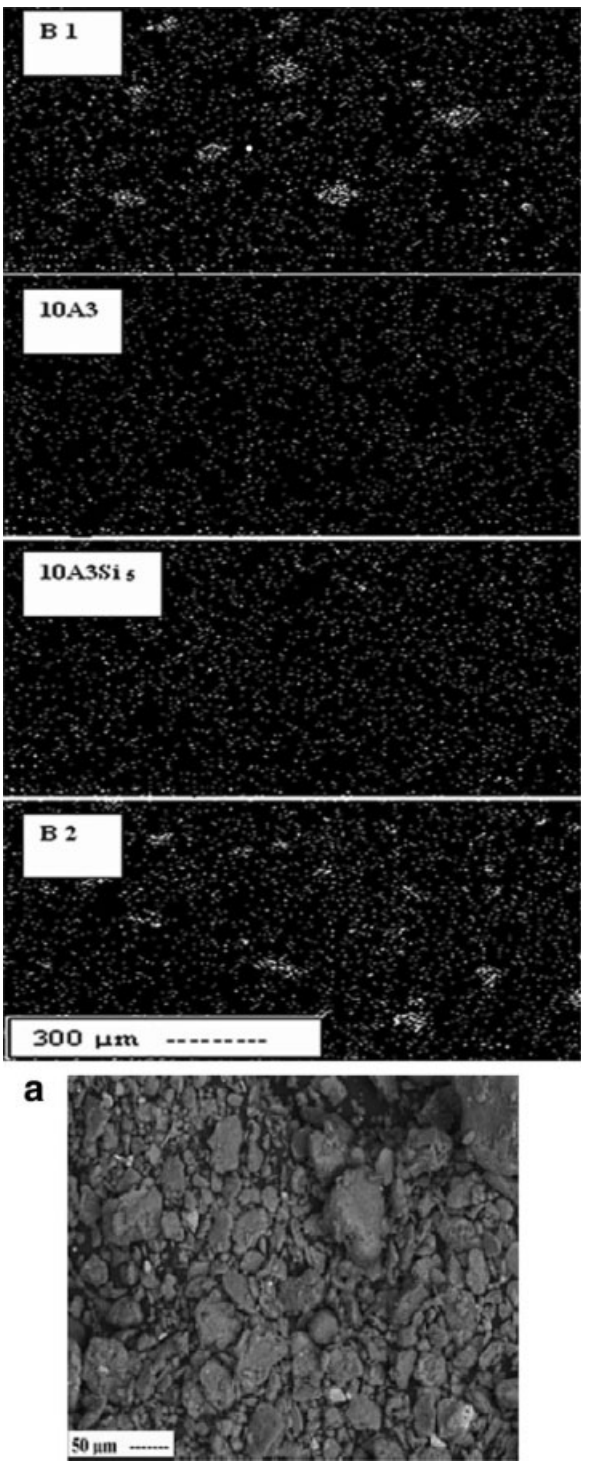

Figure 6 Al mapping of compounds by EDS, (a) SEM image of Bentonite clay.

RESULT AND DISCUSSION

Dispersion morphology of SBR/clay nanocomposite

WAXD study

Figure 1 shows the X-ray diffraction patterns of bentonite clay, compounds B2, $10A3S1_5$, and 10A3,

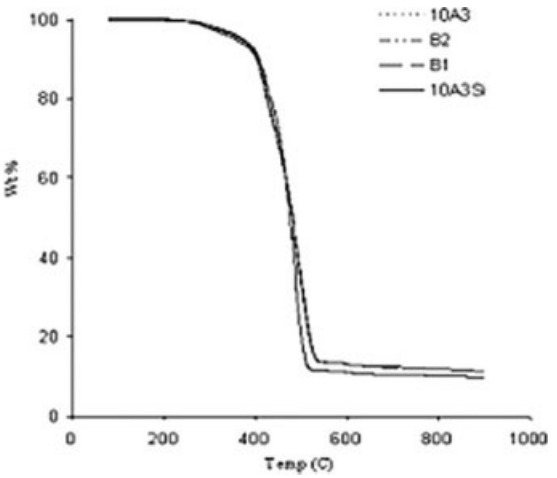

Figure 7 TGA thermogram of the compounds.

respectively. Bentonite clay shows a characteristic diffraction peak at $2\theta \sim 7.2^\circ$ corresponding to an inter-gallery distance of 1.23 nm. Compound B2 did not exhibit any shift in the diffraction peak and thus the inter-gallery distance in compound B2 remained the same as in case of bentonite clay. It can be deduced that the addition of silane in the bentonite clay gave rise to the formation of a conventional composite at a microscopic level, where polymer was not intercalated into the silicate galleries. It was expected as there were few number of silinol groups at the edge of the montmorillonite. The silinol groups can react with silane to increase the miscibility with rubber but does not effect the inter layer spacing.[23] In case of compound 10 A3, the XRD diffraction patterns were nearly flat with hump at 4.7° corresponding to a layer spacing of 1.88 nm. The intercalation of the polymer and partial exfoliation of the clay layers led to disordering of the layered clay structure causing the decrease in the XRD

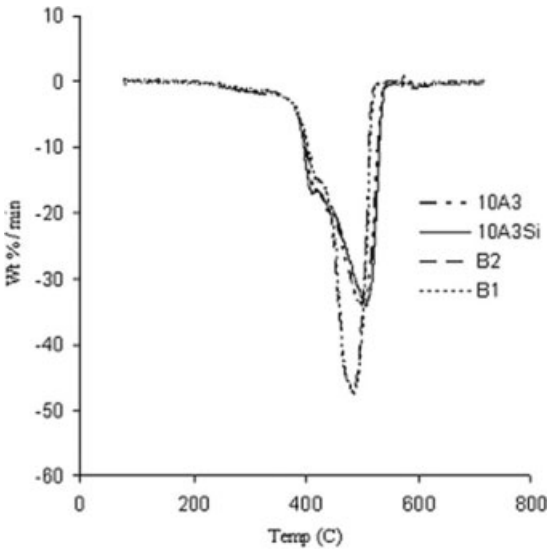

Figure 8 DTGA thermogram of the compounds.

TABLE IV
Rheometric Property of the Compounds with Varying Dose of Silane

Parameter	$5A3Si_2$	$5A3Si_5$	$5A3Si_7$	$5A3Si_{10}$
Maximum torque (T_{max}), (dN-m)	8.5	9.9	10.1	9.7
Minimum torque (T_{min}), (dN-m)	1.8	2.4	2.4	2.0
ΔTorque $= T_{max} - T_{min}$, (dN-m)	6.7	7.5	7.7	7.9
t_{s2} (min)	4.5	3.9	3.0	2.7
t_{c90} (min)	13.0	14.0	14.3	14.7
CRI (min^{-1})	11.8	10.1	8.8	8.3

coherent layer scattering intensity of the compound 10A3. Similarly, in case of compound $10A3Si_5$, the inter layer spacing remained unchanged to 1.88 nm.

TEM study

The TEM micrograph of compound 10A3 shown in Figures 2 and 3 clearly points out the exfoliated as well as the intercalated nature of the SBR bentonite clay nanocomposite. Totally exfoliated clay particles can be seen at the upper left corner of the TEM micrograph, whereas the intercalated clay particles at the middle of the micrograph. TEM photograph of compound $10A3Si_5$ shown in Figures 4 (low magnification) and 5 (high magnification) indicates the nano-scopic distribution of the clay particles in to the matrix and also the exfoliated/intercalated nature of the composite. There is basically no morphological change.

SEM–EDS study

Figure 6 compares the Al mapping of compounds B1, 10A3, $10A3Si_5$, and B2, respectively. It is evident that there is significant amount of bigger

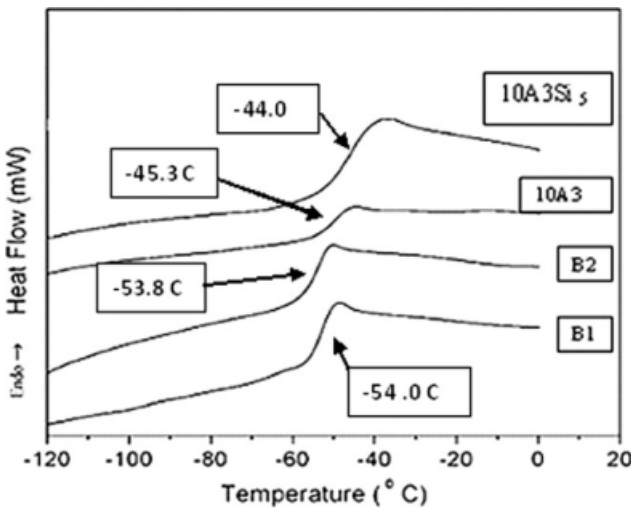

Figure 9 DSC thermogram of the compounds.

TABLE V
Rheometric Property of the Compounds with Different Formulations

Parameter	B1	B2	$10A3_{1.5}$	$10A3Si_5$	$N10_{330}$	$N10_{660}$
Maximum torque (T_{max}), (dN-m)	6.5	7.4	8.6	10.1	9.3	10.2
Minimum torque (T_{min}), (dN-m)	1.3	0.8	1.7	1.7	0.9	0.9
ΔTorque = $T_{max} - T_{min}$, (dN-m)	5.2	6.6	6.9	8.4	8.4	9.3
t_{s2} (min)	15.2	7.7	2.8	2.6	8.37	8.0
t_{c90} (min)	26.1	22.2	8.1	13.9	15.38	14.9
CRI (min^{-1})	9.2	6.8	18.9	8.8	14.3	14.5

aggregation of the bentonite clay in B1. However, the size of the clay aggregates is relatively smaller in compound B2. This was due to the miscibility effect of the silane. However, the Al signals from 10A3 and 10 $A3Si_5$ prove the homogeneous distribution of the bentonite clay is in the SBR matrix.

Si mapping of the compounds were not collected as the silane itself contains Si, which may lead misinterpretation. The magnification of the pictures were low enough (300 μm) and thus can be taken as the representative picture for the whole sample. The SEM image of the bentonite clay is shown in Figure 6(a). The image clearly points out the plate like nature of the bentonite clay.

Effect of clay on thermal behavior

TGA study

The TGA and DTG curves of the compounds B1, B2, 10A3, and $10A3Si_5$ are compared in Figures 7 and 8, while the decomposition up to 400°C, the peak decomposition temperatures and the corresponding peak decomposition rates for the compounds are tabulated in Table III. The decomposition amount up to 400°C (onset decomposition) was similar for all the compounds. It was very hard to tell any difference from TGA. However, from the peak decomposition temperature and from decomposition rate, better thermal stability of the nanocomposites can be ascertained. The peak decomposition temperature followed the trend $10A3/10A3Si_5 > B1/B2$ and exact reverse trend was followed for the peak decomposition rate (i.e $B1/B2 > 10A3/10A3Si_5$). Thermal stability of compound 10A3 and $10A3Si_5$ was comparable. Similarly, thermal stability of compound B1 and B2 was comparable. Compound B contained ordinary bentonite clay and thus formed conventional composite with very low degree of dispersion having large aggregates. Even the silane treatment did not help much to increase the distribution. Compound 10A3 and 10A3 Si_5 contained the *in situ* sodium activated and organo-modified nanocomposites. The nanocomposites helped to achieve the higher thermal resistance due to relatively better exfoliation and/or intercalation of the SBR rubber in to the clay gallery. The better thermal stability can be attributed to the carbonaceous char formed and the structure of the clay minerals. The multiplayer clay structure acts as an excellent insulator and barrier for the mass transfer.

DSC study

Dynamic DSC scans for the samples are shown in Figure 9. The glass transition (T_g) temperature of compound B1 and B2 was observed at ~ -54°C, while 10A3 and 10A3 Si_5 exhibited T_g at ~ -45.3 and -44°C, respectively. The shift in 'T_g' can be explained by the restricted mobility of the SBR chains within the bentonite layers thereby proving the intercalated/exfoliated nature of the SBR/ODA modified bentonite clay nanocomposites.[24] Thus in case of compound 10A3, effective intercalation and/or exfoliation of the of the clay has increased the T_g. Further increase of T_g values was observed in silane treated compound. This was due to more restricted mobility of the SBR chains within the bentonite layers and in the close vicinity of the clay particles through silane coupling.

Cure kinetics

Compound with different dose of silane

It is very much essential to understand the optimum dose for silane. Insufficient amount of silane will produce inadequate interaction of the silica/silicate with the rubber while higher amount of silane will unnecessarily increase the modulus and hardness of the compound. This is due to release of free sulfur from the excess amount of silane. Moreover, the cost of silane is also a factor.

The cure property of the compounds with different dose of silane are compiled in Table IV. The extent of curing (given by the ΔTorque values) is highest in compound $10A3Si_{10}$ followed by compound $10A3Si_7$, $10A3Si_5$, and $10A3Si_2$. This was due to effective chemical bond formation of SBR rubber chains with the silinol groups of the clay through silane coupling agent. This leads to better rubber-to-filler interaction. It was observed that with the increase of the silane content, the scorch safety of the compounds (t_{s2}) decreases. This was due to early break down of the silane, which released sulfur for curing. However, it was observed that with the increase of

TABLE VI
Physical Properties of Compound with Varying Dose of Silane

Parameter	$5A3Si_2$	$5A3Si_5$	$5A3Si_7$	$5A3Si_{10}$
50%modulus (MPa)	0.9[a]	1.0	1.0	1.0
300%modulus (MPa)	3.6	3.9	4.1	5.5
Tensile strength (MPa)	6.8	7.5	7.9	6.2
EB (%)	470	423	412	400
Hardness (S)	51.5	53.0	54.0	55.0
Swelling index	4.18	4.15	4.00	3.85
Volume fraction	0.170	0.172	0.183	0.190
Tear strength (N/mm)	19.2	30.4	32.6	25.2
Bound rubber (%)	18.2	20.1	22.0	22.7

[a] The tensile and tear properties of the compounds are the mean of five measurements and the rest properties are the average of the two measurements.

the silane, the t_{c90} (time required to reach the 90% to the maximum torque) value of the compound increases and that of CRI decreases. This was due to interaction of the silane with sulfonamide accelerator[25] or interaction of the silane with octadecyl amine present in the clay and thus reduced the accelerating effect of the amine groups.[26]

Compounds with different formulations

It was observed that the ΔTorque value of $10A3Si_5$ was comparable with $N10_{330}$ and $N10_{660}$. The ΔTorque value of compound 10A3 was lower in comparison to $10A3Si_5$ but was higher in comparison to B1 or B2. This was due to strong reinforcing effect of the organoclay. It is of interest to point out that the addition of silane has increased the ΔTorque value further. This was due to higher compatibility at the elastomer–filler interface. The t_{s2} value of compound B2 was lower in comparison to B1. Similarly, compound $10A3Si_5$ exhibited lower t_{s2} value compared to 10A3. The reason has been explained earlier. However, the presence of octadecyl amine drastically reduced the t_{s2} value in 10A3 or $10A3Si_5$ in comparison to B1, B2, $N10_{330}$, and $N10_{660.}$ This is expected as amines are regarded as scorchy accelerator.[27]

It was observed that the addition of silane increased the t_{c90} and thus the CRI value. This was due to interaction of the silane with sulfonamide accelerator or with octadecyl amine present in the clay as explained earlier.

The properties are reported in Table V.

Physical property

Compounds with varying dose of silane

Physical property of compounds having different amount of silane have been reported in Table VI. It was observed that with increase of silane the modulus increases. This was due to the silane coupling agent, which acted as a cross-linking agent also. The silane increases the cross link density of the compound, thereby enhancing the modulus of the compounds. This was supported by the higher hardness and lower elongation of the compounds. The swelling index and volume fraction followed the opposite trend. Bound rubber content also increases with increase of silane content. Increase in bound rubber content is an indication of increase of compatibility between rubber and clay. At a glance, the properties reached to optimum level at 5% silane content with respect to clay loading.

Compounds with different formulations

Physical properties of different compounds have been reported in Table VII. The mechanical properties, viz., 50 and 300% modulus and tensile strength is higher

TABLE VII
Physical Properties of Different Compounds

Parameter	B1	B2	10A3	$10A3Si_5$	$N10_{330}$	$N10_{660}$
50% modulus (Mpa)	0.7 (0.9)[a]	0.7[b] (1.0)	1.62 (1.8)	1.7 (1.9)	0.74 (0.78)	1.02 (1.5)
300% modulus (Mpa)	1.8 (2.0)	3.3 (3.5)	4.2 (4.98)	6.3 (6.5)	3.1 (4.1)	3.2 (3.6)
Tensile strength (Mpa)	2.8 (2.4)	3.9 (3.5)	8.2 (10.11)	9.5 (8.2)	8.4 (6.8)	5.8 (4.0)
Elongation at break (%)	341 (311)	384 (350)	544 (500)	394 (350)	525 (394)	405 (280)
Hardness (S)	44 (47)	46 (48)	52 (54)	53 (56)	50 (51)	48 (50)
Swelling index	5.12	4.80	4.61	4.43	4.35	4.35
Volume fraction	0.158	0.169	0.175	0.183	0.188	0.188
Tear strength (N/mm)	13.0	16.0	26.0	30.6	30.6	25.0
Bound rubber (%)	12.3	16.4	22.0	26.7	20.1	18.2
Rebound resilience (%)	68.5	67.2	55.6	60.0	65.9	68.0
Compression set (%) @ 105 C/24 h	35.0	32.0	53.4	31.5	37.8	31.4
Mooney viscosity ML (1 + 4) @ 100°C	46.2	51.2	59.7	80.2	50.0	48.4
FTFT (Kcys)	7.6	9.1	25.9	50.3	30.1	29.4
Air permeability (m^2/Pa-sec)	2.25	2.10	1.50	1.53	2.22	2.11

[a] The result in parenthesis represents the aged property.
[b] The tensile and tear properties of the compounds are the mean of five measurements and the rest properties are the average of the two measurements.

in compound 10A3 in comparison to compound B1,B2, $N10_{330}$, and $N10_{660}$. The more effective intercalation and/or exfoliation of the SBR chain in the organo amine-modified clay is probably responsible for the increase in tensile properties in compound 10A3 compared to the other compounds. Higher hardness of compound 10A3 was probably due to presence of organoclay. Swelling index and volume fraction followed the same trend. However, it was observed that the tear strength of compound 10A3 was $\sim$ 18% lower in comparison to high structure N330 carbon black. This was due to the weak interaction of the rubber at the edge of the plate like clay particle. Still, the tear property of 10A3 was respectively $\sim$ 50% and 38% better in comparison to B1 and B2.Compound 10A3 exhibited height elongation at break. Even after ageing, the elongation at break was considerably higher. This leads to higher tensile strength after ageing. This was due to slippage of the rubber chain from the surface of the clay particles. Other aged property of the compounds followed the same trend as that of unaged property.

The effect of silane treatment can easily be seen in compound $10A3Si_5$. The addition of silane to the *in situ* sodium activated organo modified bentonite clay as in compound $10A3Si_5$, results in a nominal increase of 5% in the unaged 50% modulus but a significant increase of $\sim$ 50% in the unaged 300% modulus over compound 10A3. A substantial increase of $\sim$ 18% in both the tensile strength and tear strength over compound 10A3 was observed. A slight 1 unit increase of Shore A hardness in comparison to compound 10A3 was found

Higher bound rubber content of compound 10A3 indicates the better rubber to filler interaction, which leads to better strength property. Compound $N10_{660}$, which contained low structure N660 carbon black, exhibited lower strength property. This was also reflected in low bound rubber content of the compound ($\sim$ 22% lower in comparison to compound 10A3).The rebound resilience of compound 10A3 was lowest among ($\sim$ 55.6) all the compounds. Compression set was highest in case of compound 10A3 ($\sim$ 53.4%). These two are the most disadvantageous property in application point of view such as tyre tread or tyre inner liner or tube. This was probably due to irreversible slippage of the rubber chain from the clay surface. It has been reported that the set and rebound property decreases in presence of organoclay. Silane treatment as in compound $10A3si_5$ improved the rebound resilience to an extent of 8% over the 10A3 compound. But, still it was inferior in comparison to $N10_{330}$ and $N10_{660}$. However, a substantial improvement of $\sim$ 40% in compression set property was observed in case of compound $10A3Si_5$ over 10A3. As expected the bound rubber content of the compound $10A3Si_5$ was highest.

The mooney viscosity of compound B1 was lowest followed by $N10_{330}$ and $N10_{660}$. This was due to lowest rubber to filler interaction in compound B1 (a conventional composite). Being a conventional composite, compound B1 exhibited lowest strength property. Adding silane in compound B2, increased to mooney viscosity by 5 unit over compound B1. Compound 10A3 had mooney viscosity of 59.7 unit and was probably due to better rubber to filler interaction. Compound $10A3Si_5$ exhibited height mooney viscosity of 80.2 unit due to strong interaction with rubber to filler through silane.

Fatigue life of compound B1 was poorest ($\sim$ 8 Kcys) due to lack of rubber filler interaction as well as presence of big particles, which were the weak points under cyclic deformation. Compound B2 exhibited slightly better fatigue life compared to B1($\sim$ 9 Kcys). It was due to relatively better interaction through silane coupling agent. $N10_{330}$ and $N10_{660}$ also showed good fatigue life of $\sim$ 30 Kcys due to strong rubber to filler interaction through physicochemical bonding. Compound 10A3 exhibited $\sim$ 15% lower fatigue life in comparison to carbon black filler compounds. However, compound $10A3Si_5$ demonstrated substantially higher fatigue life of $\sim$ 50.3 Kcys due to silane treatment.

As expected, the air retention property of compound 10A3 was much better in comparison to B1, B2, $N10_{330}$, or $N10_{660}$. This was mainly due to presence of nano-scale dispersion of the plate like clay particles in to the matrix. However, silane treatment of the organoclay did not improve the permeation property further.

Mechanism of silane treatment on *in situ* sodium activated and organo-modification bentonite clay

The reaction mechanism of silica–silane–rubber has been reported by Gorl et al.[28] The reaction proceeds through the silanol group of the silica surface and the tri-etoxy group of the silane. However, amount of silanol group in the clay is relatively small and is situated at the edge of the clay particles.[23] The silane can react with these silanol groups as well as the amines situated at the surface of the clay.[2] The interaction of the rubber with the organoclay generates from the weak van der Walls force of interaction, where as that of carbon black generates from strong physicochemical interaction. Due to absence of strong chemical interaction with the organoclay, there is a chance of slippage of rubber chain from the surface of the clay particles. This leads to higher elongation of the organoclay compounds (like 10A3). According to Mousa and Karger–Kocsis,[13] the unexpected elongation of the nanocomposites is likely due to the encapsulation of the individual clay layers and tactoids in a more cross link rubber

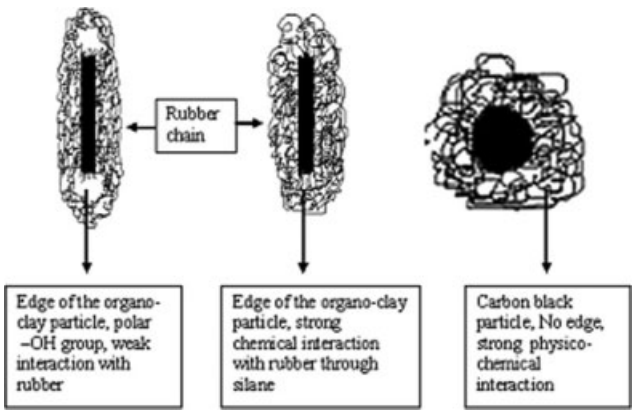

Figure 10 Interaction mechanism of rubber chain with organo- clay, silane treated organoclay, and carbon black.

fraction than the bulk itself. As a consequence, the overall elongation corresponds to that of a less cross linked rubber. The same factor is responsible for low resilience and higher compression set property of the organoclay filled compounds (10A3). However, in case of compound B1 and B2, such type of morphological change is not possible. Thus compound B1 and B2 exhibited lower elongation.

During silane treatment, a strong chemical interaction occurs through silanol–silane reaction. This leads to prevention of rubber chain slippage from the clay surface and thus lower elongation at break (like $10A3Si_5$). The coupling of the clay particle with the rubber chain through silane improves the resilience and the compression set property. The improvement of the resilience and the compression set property in $10A3Si_5$ was due to low slippage of the rubber chain from clay surface. It was found that the fatigue life of compound 10A3 was much better than B1 or B2 but was inferior in comparison to the $N10_{330}$ or $N10_{660}$. The better fatigue life of compound 10A3 over B1 or B2 can be explained based on the relatively better rubber to filler interaction. However, the carbon black is nano particles with more or less spherical nature having strong interaction with rubber. On the contrary, the interaction at the edge of the clay particles rubber is weakest As a result, during the cyclic deformation the stress concentration is highest at the edge of the clay particles. Thus, the flaws can generate easily at these points in comparison to the strongly attached nearly spherical carbon black particles. Thus, the organoclay containing compounds exhibited low fatigue life compared to black filled compound. Addition of silane in the organoclay improves the interaction at the edge of the clay particle through chemical cross linking with rubber. This type of interaction reduces the chance of flaw generation at the edge of the clay particles and thus improves the fatigue life. A pictorial presentation of the above mechanism is represented in Figure 10.

Conclusion

The study represents an effective way to tailor make the property of the conventional *in situ* sodium activated organoclay nanocomposites. Besides strength property, some times it is required that the compound should have higher viscous component (like racing tyre tread component), which is reflected by lower rebound and higher compression set. Some times these properties are unwanted (like tube compound). Treatment of silane has improved the rebound resilience and compression set property over the conventional *in situ* sodium activated organo modified bentonite clay nanocomposites. Moreover, silane treatment has drastically improved the fatigue life. This is one of the most critical requirements for rubber compound as in tyre tread, side wall, or tube. Silane treated compound has also shown higher modulus, tensile, and tear property.

The authors thank HASETRI and JK Tyre management for kind permission to publish this work.

References

1. Pramanik, M.; Srivastava, S. K.; Samantaray, B. K.; Bhowmick, A. K. J Appl Polym Sci 2003, 87, 2216.
2. Ganter, M.; Gronski, W.; Reichert, P.; Mulhaupt, R. Rubber Chem Technol 2001, 74, 221.
3. Ganter, M.; Gronski, W.; Semke, H.; Zilg, T.; Thomann, C.; Mulhaupt, R. Kautsch Gummi Kunstst 2001, 54, 166.
4. Kojima, Y.; Fukumori, K.; Usuki, A.; Okada, A.; Kurauchi, T. J Mater Sci Lett 1993, 12, 889.
5. Vu, Y. T.; Mark, J. E.; Pham, L. H.; Engelhardt, M. J Appl Polym Sci 2001, 82, 1391.
6. Arroyo, M.; Lopez-Manchado, M. A.; Herrero, B. Polymer 2003, 44, 2447.
7. Lopez-Manchado, M. A.; Arroyo, M.; Herrero, B.; Biagiotti, J. J Appl Polym Sci 2003, 89, 1.
8. Teh, P. L.; Mohd Isak, Z. A.; Hashim, A. S.; Karger-Kocsis, J.; Ishiaku, U. S. J Appl Polym Sci 2004, 94, 2438.
9. Varghese, S.; Karger-Kocsis, J. J Appl Polym Sci 2004, 91, 813.
10. Teh, P. L.; Mohd Isak, Z. A.; Hashim, A. S.; Karger-Kocsis, J; Ishiaku, U. S. J Appl Polym Sci 2006, 100, 1083.
11. Sengupta, R.; Sabharwal, S.; Bhowmick, A. K.; Chaki, T. K. Polym Degrad stab 2006, 91, 1311.
12. Jia, Q.-X.; Wu, Y.-P.; Xu, Y.-L.; Mao, H.-H.; Zhang, L.-Q. Macromol Mater Eng 2006, 291, 218.
13. Karger-Kocsis, J.; Wu, C.-M. Polym Eng Sci 2004, 44, 1083.
14. Varghese, S.; Karger-Kocsis, J. Polymer 2003, 44, 4921.
15. Wang, Y.; Zhang, H.; Wu, Y.; Yang, J.; Zhang, L. J Appl Polym Sci 2005, 96, 318.
16. Stephen, R.; Alex, R.; Cherian, T.; Varghese, S.; Joseph, K.; Thomas, S. J Appl Polym Sci 2006, 101, 2355.
17. Zhang, L.; Wang, Y.; Wang, Y.; Sui, Y.; Yu, D. J Appl Polym Sci 2000, 78, 1873.
18. Wang, Y.; Zhang, L.; Tang, C.; Yu, D. J Appl Polym Sci 2000, 78, 1879.
19. Dias, A. J.; Jones, G. E.; Tracey, D. S.; Waddell, W. H. Exxon Mobil Chemical Company, PCT No- PCT/US01/42767291, Int Cl- C08L 27/00, US Cl.- 524/515, US 2004/0132894A1 (2001).

20. Heinrich, G.; Herrmann, W.; Kendziorra, N.; Pietag, T.; Recker, C. Continental Aktiengesell-Schaft, Int.Cl-C08K 3/34, U.S Cl.- 524/442; 524/236, U.S. Pat. 2002/0095008A1 (2001).
21. Chakraborty, S.; Sengupta, R.; Dasgupta, S.; Mukhopadhyay, R.; Bandoypadhyay, S.; Joshi, M.; Ameta, S. C. J Appl Polym Sci 2009, 113, 1316.
22. Gent, A. N.; Hartwell, J. A. Rubber Chem Technol 2003, 76, 517.
23. Utracki, L. A. In Clay Containing Polymeric Nanocomposites, 1st ed.; Rapra Technology: Shawbury, UK, 2004; Vol 1, Chapter 2.2, p 95.
24. Lopez-Manchado, M. A.; Herrero, B.; Arroyo, M. Polymer Int 2003, 52, 1070.
25. Adhukari, A.; Mukhopadhyay, R. Presented at the International Rubber conference- 1992, Beijing, China, Oct 13–15, 1992.
26. Lopez-Manchado, M. A.; Herrero, B.; Arroyo, M. Polymer Int 2004, 53, 1766.
27. Eirich, F. R. In Science and Technology of Rubber, 1st ed.; Academic press: New York, 1978; Chapter 7, p 299.
28. Gorl, U.; Parkhouse, A. Kautsch Gummi Kunstst 1999, 52, 493.